JOINT INSTITUTE FOR NUCLEAR RESEARCH
Frank Laboratory for Neutron Physics

FINAL REPORT ON THE INTEREST PROGRAMME

Coexistence of Superconductivity and Ferromagnetism at Low-Dimensional Heterostructures

Supervisor:
Dr. Vladimir Zhaketov

Student:
Ervin Naufal Arrasyid,
Bandung Institute of
Technology

Participation period:
27 September- 05 November
2021, Wave 5

Dubna, 2021

Abstract

Proximity effect is an effect which occurs mainly in superconductor-ferromagnet (S/F) layers and its respective heterostructures. Historically, superconductivity was thought to be devoid of ferromagnetism and vice versa. However, tuning superconducting order parameter for S/F geometry has predicted the existence of proximity effect and its inverse proximity effect. Proximity effect can be measured using neutron polarized reflectometry where scattered neutron beam intensity could be compared above and below superconducting critical temperature to observe spin asymmetry existence. REMUR reactor is a powerful reactor equipped with spin flippers device which enabled spin asymmetry measurement. In this project, we did several tasks on sapphire/Nb/Gd/V/Nb heterostructres and simulate neutron and xray reflectivity of this sample. Besides that, real experiments data is also processed and compared with simulation results. There are differing results between experimental data and simulation results which could be attributed to some systemic error hampered by incorrect initial value input. Nonetheless, spin asymmetry results showed the existence of proximity effect due to increase of asymmetry which translated into suppressed ferromagnetism due to spilling of Cooper pair coherence inside ferromagnetic layer.

Introduction

Superconductivity

Superconductivity was discovered by Heike Kamerlingh Onnes on April 8th, 1911, after he measured vanishing resistance of elemental mercury (Hg) below 4.2K. There was no physical interpretation which explained the cause of superconductivity until the advent of Barden-Cooper-Schrieffer (BCS) theory in 1957. On this day, Onnes also discovered superfluidity by noticing a boiling of He-4 below 2K and a jump of heat capacity by a factor of 10^5. Only latter in 1938 that Russian scientist Pyotr Kapitsa and John Allen discovered zero resistance flow in He-4 below 2K and gave superfluidity its name [1].

Both superconductivity and superfluidity were some of the earliest examples of phase transition phenomena that happened due to quantum nature of electron due to coherence of wavefunction of electrons in ground state below their phase transition temperature (T_c). Superconductivity and superfluidity transition were also early examples of new phases of matter discovered beyond thermodynamics phases of matter and ferromagnetic phases of matter which famously occurred below Curie's Temperature (T_C). In nature, there are only 4 materials that has T_C beyond 273 K which are iron (1043 K), cobalt (1394 K), nickel (631 K), and Gadolinium (292 K) [2].

Aside from zero resistance, superconductivity has perfect diamagnetism in the sense that there was no magnetic field inside superconductor, and it expulsed external magnetic fields until certain field values (H_c). This property was named after its discoverer, Meissner effect. Above H_c superconductivity vanished except for Type-II superconductor where above H_c , superconductivity existed with supercurrent vortex where it pinned magnetic field until

certain values. Superconductivity vanished completely beyond it (Hc_2). This phase is called Abrikosov phase, named after Russian scientist Alexei Abrikosov, who discovered it. All elemental superconductors have T_c below 10 K such as Niobium (T_c=9.26K, H_c=0.82T, type-II), Vanadium (T_c=5.03K, H_c=1T, Type-II), and Lead (T_c=7.19K, H_c=0.08T, type-II). Compound usually has a larger T_c and H_c and usually has type-II superconductivity such as Nb_3Ge (T_c=23.2K, H_c=37T), MgB_2 (T_c=39K, H_c=74T), and Nb_3Sn (T_c=K, H_c=30T) [3].

All superconductors discovered until 1980 had maximum T_c around 40K. After 1986 many superconductors with temperatures beyond 77K (boiling point of N_2) were discovered and were mainly cuprates-oxide based superconductors. These superconductors were two-dimensional heterostructures and had perovskite lattice structure with orthorhombic geometry of unit cell. The compound such as YBCO (T_c=95K), BSCCO (T_c=95K), HgTiBaCaCaCuO (T_c=164K) are type two superconductors and colloquially called as High-T_c superconductors. In 21st century, iron-based superconductors were discovered such as FeSe (T_c=65K), SmFeAs(O,F) (T_c=55K), and CeFeAs(O,F) which was unprecedented due to incompatibility of superconductivity with ferromagnetism. All compounds mentioned in this paragraph are unconventional superconductors where microscopic phenomena which gave rise to superconductivity could not be described by BCS theory.

Microscopic theory BCS relied on the assumption that as electron passes through crystal lattices it polarized electron cloud in the lattice and in doing so it made lattice distortion which took time to relax. If a second electron passed the lattice before the distortion relaxed, then it would have a lower energy because the lattice was polarized. As such, it would have attractive interaction between the two electrons forming Cooper pair and such attractive force is called Froehlich interaction. Froechlich interaction is a phonon mediated interaction between electrons with opposite spins which lower the energy of Cooper pair, and it has a lower energy that the energy of two electrons combined, thus favoring pairing. The treatment of BCS theory would not be provided here. In superconductivity, macroscopic explanation of zero resistivity and Meissner effect can be invoked through a parameter known as *supercurrent density* which was derived from current density formulation in quantum mechanics,

$$\vec{J_s} = \frac{q^*}{2m^*}\left\{\Psi^*\left(\frac{\hbar}{i}\vec{\nabla} - \frac{q^*}{c}\vec{A}\right)\Psi + \left[\left(\frac{\hbar}{i}\vec{\nabla} - \frac{q^*}{c}\vec{A}\right)\Psi\right]\Psi^*\right\}$$

Where $q^* = -2|e|$ is charge of Cooper pair, $m^* = 2m_o$ is the effective mass of Cooper pair and $\vec{A}$ is vector potential which is added to momentum operator due to gauge invariance of momentum operator in the presence of magnetic field. Ψ is superconducting order parameter which is introduced by Russian scientists Vitaly Ginzburg and Lev Landau and took the form of

$$\Psi(\vec{r}) = |\Psi(\vec{r})|e^{i\theta(\vec{r})} = [n_s^*]^{\frac{1}{2}}e^{i\theta(\vec{r})}$$

Where n_s^* is the number of Cooper pair in the sample which is easily in the order of 10^{23}. If we input this order parameter into supercurrent density and using some Algebra, the following supercurrent equation can be described,

$$\vec{J_s} = -\frac{\vec{A}}{\Lambda_s c} + \frac{\hbar}{q^* \Lambda_s}\vec{\nabla}\theta$$

Where $\Lambda_s = m^*/(q^{*2} n_s^*)$. If we assume that Cooper pair density is independent of time, then time differentiation of the supercurrent equation would yield,

$$\vec{E} = \Lambda_s \frac{\partial \vec{J_s}}{\partial t}$$

Since m^* is so small and n_s^* so large, then the value of current is nearly infinite. If we took the curl of supercurrent equation and invoke a little bit differentiation and maxwell equation,

$$\vec{\nabla} \times \vec{J_s} = -\frac{1}{\Lambda_s c}\vec{B}$$

Knowing, that $\vec{\nabla} \times \vec{H} = (4\pi/c)\vec{j}$ and $\vec{B} = \hat{\mu}\vec{H}$

$$\vec{\nabla} \times \vec{\nabla} \times \vec{B} = \vec{\nabla}\left(\vec{\nabla} \cdot \vec{\mathrm{B}}\right) - \nabla^2 \vec{\mathrm{B}}$$

Since $\left(\vec{\nabla} \cdot \vec{\mathrm{B}}\right) = 0$

$$\nabla^2 \vec{\mathrm{B}} = \frac{1}{\lambda_s^2}\vec{\mathrm{B}}$$

Where λ_s is the superconducting penetration depth and it has the values of,

$$\lambda_s = \left(\frac{\Lambda_s c^2}{4\pi\hat{\mu}}\right)^{\frac{1}{2}} = \left(\frac{m^* c}{4\pi\vec{\nabla} q^* n_s^*}\right)^{\frac{1}{2}}$$

The above equation that relates zero resistivity and superconducting penetration depth are called as first and second London equation. The solution for the second London equation can be written as

$$B(z) = B(0)e^{\left(-\frac{z}{\lambda_s}\right)}$$

Which manifest that magnetic field is suppressed inside superconductor, at least not until penetration depth which has order in several dozens or hundreds nm. For this reason, it was thought until the early 1980s that superconductivity would not happen if it was composed of magnetic materials, hence the discovery of iron-based superconductors and superconductivity-ferromagnetism proximity effect initially baffled many scientists. Further derivations of London equation would give *coherence length* or the Cooper pair correlation

length in absence of any scattering. In short, electrons in any distance below this length could interact as pair.

$$\xi_o = \frac{h v_F}{\pi \Delta_o}$$

Where v_F is Fermo velocity and $\Delta_o = m^* v\, \delta v$ [3].

Proximity Effect and Inverse Proximity in Superconductor-Ferromagnet

As previously mentioned, ferromagnetism could destroy superconductivity due to the existence of external field, as such for a long time it was thought that ferromagnets were not compatible to become superconductor. Vitaly Ginzburg formulated this problem which explained the problem which concluded that ferromagnet would suppress superconductivity. In Frohlich interaction, minimization of energy in superconductors happened because interaction of an electron with momentum $\overrightarrow{k_1}$ gave rise to lattice polarization (phonon) with momentum $\overrightarrow{k_1'}$ and it interacted with second electron with momentum $\overrightarrow{k_2}$ and its respective phonon with momentum $\overrightarrow{k_2'}$. The interaction is such that,

$$\overrightarrow{k_1} + \overrightarrow{k_2} = \overrightarrow{k_1'} + \overrightarrow{k_2'} = 0$$

From the equation above, it was clear that interaction only occurs if and only if the electron occurred to have opposite momentum. In broader term, interaction in cooper pair is maximized if the electron occurred to have opposite total momentum and hence opposite spin. After the invent of BCS theory, it was firmly believed that in conventional superconductor, exchange interaction of ferromagnet would align spin of cooper pair and as such decrease the coherence of superconducting states by increasing the pairing energy inside superconductor. However, Paul Anderson displayed that ferromagnetism would not arise inside superconductor because spin alignment happened in short-range, and it mainly happened for ion-core and the effect was negated by long-range interaction of coherence length. Instead, Anderson argued that non-ordered magnetic would appear in superconductor and this new state was called cryptoferromagnet. In unconventional superconductor such as UGe_2, ferromagnetism is observed as bulk properties of the sample. This occurred due to the pairing of three electron forming triplet pair and such could not be treated using BCS theory [4].

Following the definition of superconductor where a material has zero electric resistance and expelling external magnetic field, it was easy to explain why ferromagnetism would not arise in superconductivity. Meissner effect prevent field to enter and affect Cooper pair. However as mentioned before, magnetic field could enter superconductor and caused the existence of superconductor vortex. Cooper pair would not be easily affected by external magnetic field if the penetration depth of magnetic field (λ_s) is smaller than superconductivity coherence length (ξ_o). This assumption was true for bulk superconductors but for 2-D heterostructures consisted of ferromagnet(F) and Superconductors (S) layers, cooper pair of superconducting layers could penetrate in a damped situation in ferromagnet (proximity effect) and vice

versa where ferromagnetic ordering happened inside superconductor (inverse proximity effect). Both effects happened due to the small dimensional thickness of the layer compared to superconductor penetration depth (λ_s) as well as coherence length (ξ_o), as a result magnetic field could penetrate well inside the superconductor and vice versa, electron in superconductors could perturb and affect electron in ferromagnetic layer and gave rise to pairing in ferromagnet layer. There are many effects related to this phenomenon like spatial oscillations of density of states of electron, a nonmonotonic dependence of critical temperature of S/F layer/multilayers [5].

In zero magnetic field, electron paired in Cooper pair is formed by two electrons with opposite momenta. However, in the presence of magnetic field, Zeeman splitting occur, and momentum of the electron would shift by the value of $+\delta k = \mu_B H/v_F$ and as such we would get $\overrightarrow{k_1} + \overrightarrow{k_2} = 2\delta k \neq 0$. Cooper pair in this state is called FFLO state named after Fulde, Ferrel, Larkin, Ovchinnikov. The treatment of FFLO state is performed using Ginzburg-Landau order parameter functional, which is tuned to the geometry of the system and very difficult to be parametirized. For a very simple S/F layer the functional took form of,

$$a\psi - \gamma \frac{\partial^2 \psi}{\partial^2 x} + \frac{\eta}{2} \frac{\partial^4 \psi}{\partial x^4} = 0$$

The solution for above equation is oscillating order parameter $\psi = \psi_o \exp(kx)$ with a complex wave vector $k = k_1 + ik_2$ where k_1 and k_2 are momentum for each electron. If we assume that the order parameter in superconductor to be real, then order parameter of ferromagnet is also real,

$$\psi(x) = \psi_i \exp(-k_1 x) \cos(k_2 x)$$

The above equation showed that superconductor order perimeter exists in ferromagnet albeit in an oscillating and damped form. Nonetheless, FFLO states showed that proximity effect could occur in S/F layer. Since order parameters is correlated with density of states, this equation also showed how superconductivity density of states exist, and oscillating, inside ferromagnet. In superconductor, which is in contact with ferromagnet, it received magnetization with value of

$$\delta M = 2\mu_B N_0 \pi k_B T \sum_{n>0} \boldsymbol{g}(\boldsymbol{x}, \boldsymbol{\omega_n})$$

Where g is normal Green function over x and Matsubara frequency [6].

Polarized Neutron Reflectivity

In this experiment, polarized neutron spectrometer REMUR in Dubna is being used to characterize heterostructures samples [7]. One feature of reflectometry mode in REMUR reactor is that it has spin-flippers tool which allowed observation of spin asymmetry, $SA = \frac{R_+ - R_-}{R_+ + R_-}$ that might arise such as in proximity effect of superconductivity. Suppression of ferromagnetism due to spilling of cooper pair inside ferromagnet could be deduced by comparing spin asymmetry of S/F heterostructures above and below superconducting

transition temperatures [8]. The difference in asymmetry could be attributed to electromagnetic origin. The setup has been used to setup experiments in proximity effects in SF heterostructures composed of Gd/Nb layers, V/Fe0.7V0.3/V/Fe0.7V0.3/Nb and Nb/Ni0.65(0.81)Cu0.35(0.19), Dy/Ho thin films, and V (40 nm)/Fe (1 nm) layers [9–12].

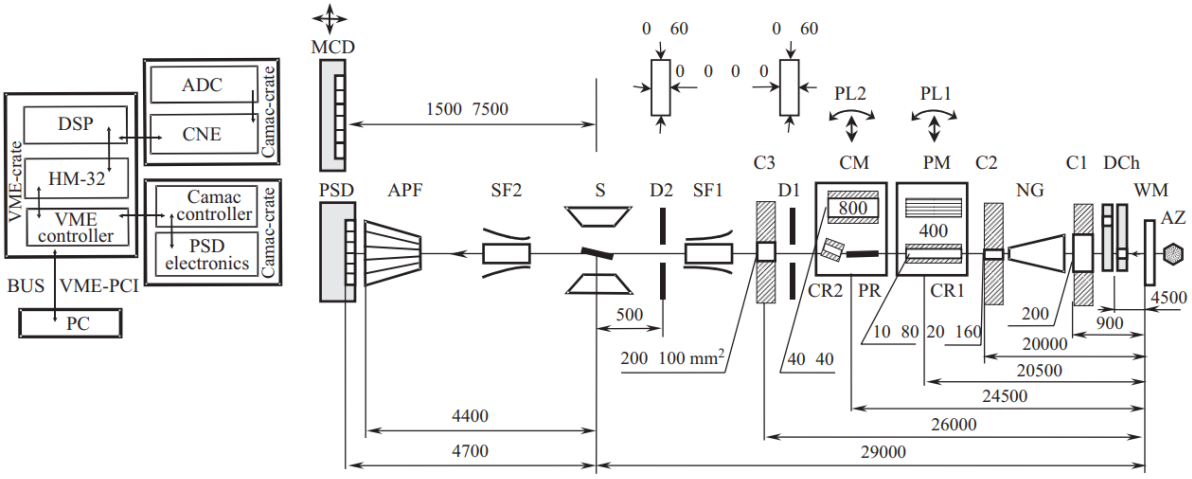

Figure 1. Schematic diagram of polarized neutron reflectivity used in the experiment

Methods and Goals

The main purpose of this project was to study and determine X-Ray Reflectivity and Neutron Reflectivity using both experimental results and simulation from heterostructures which were composed of niobium (Nb), gadolinium (Gd), Vanadium (V), sapphire substrate (Al_2O_3), and another element. In this project, there were several software which was utilized to simulate and calculate numerical value. To open and extract numerical data of the neutron reflectometry experiment, Spectra Software was used. X'Pert Reflectivity from PANanalytical was being used to simulate X-Ray reflectivity from heterostructures layers. In addition to that, numerical calculation and simulation of neutron reflectivity was performed using MatLab using Lemur.m file being provided by Dr. Zhaketov. Finally, plotting and several calculations was carried out using OriginLab. All magnetization values in the sample were in Oe.

Task 1

In the first task, experimental data of two neutron reflectometry experiments (T=12K (above T_c) and T=1.5K (below T_c)) was extracted from Spectra Sofrware and its numerical value (both during spin flipper on (-) and off (+)) was exported to Origin. Then, reflectivity of the samples could be determined from knowing that $R_+ = I_+/I_{dir}$ and $R_- = I_-/I_{dir}$ where R denotes reflectivity for flipper on (-) and flipper off (+) condition. I_{dir} was reference spectra or Maxwell spectra from the experiment. After that, it was imperative to calculate spin asymmetry from the experimental data using equation $SA = (R_+ - R_-)/(R_+ + R_-)$, where

SA symbolizes spin asymmetry for each wavelength. Wavelength of the experimental data can be determined by equation below,

$$\lambda[\text{Å}] = \frac{(N + 35 - 12) * 3.956 * 256}{34030}.$$

After performing calculation and plotting of experimental data, neutron reflectivity data was compared with simulation using lemur program in Matlab. The simulation was because below T_c superconducting layers close to ferromagnet layer was magnetized and at the same time ferromagnetism in ferromagnetic layer was suppressed due to proximity effect while above T_c ferromagnetism was not suppressed, and superconducting layer was not magnetized. Reflectivity data (flipper on (-) and flipper off (+) condition) from simulation and their respective spin asymmetry was compared with experimental data. The fitting was carried out by determining the correct layer number and magnetization value occurred inside the layers. In this simulation the following layers and 7.6mrad grazing angle of neutron were the basis for simulation.

$$Al_2O_3/Nb/Gd/V/Nb$$

Task 2

The second task was comparing neutron reflectivity simulation using lemur software with respect to varying grazing angles (θ = 3 mrad, 6 mrad, 12 mrad). In this task, it was assumed that there was no magnetization occurring in the layers. Basis layers were:

Al_2O_3/Nb (100 nm)/Gd (3 nm)/V (70 nm)/Nb (15 nm)

Task 3

In this task, neutron reflectivity at different magnetization value was compared. It assumed constant neutron grazing angle for each simulation (6 mrad). The magnetization being compared is differentiated into collinear case (M_x and $M_y = 0$) and non-collinear case (M_x / $M_y \neq 0$). In summary, the variables of the simulations were:

Case	Mz	Mx	My
Collinear	100, 1000, 10000 Oe	0 Oe	0 Oe
Non-Collinear	1000	100, 500, 1000 Oe	0 Oe

Furthermore, similar with previous task, it was assumed that the layers were as follow:

Al_2O_3/Nb (100 nm)/Gd (3 nm)/V (70 nm)/Nb (15 nm)

Task 4

For this task, reflectivity simulation of neutron using Lemur program and X-Ray reflectivity simulation using X'Pert Reflectometry software were carried out with a new variable, thickness. It was assumed that there was no magnetization, and the grazing angle of neutron was 6 mrad. There are three thickness variations in Gd layers:

Al_2O_3/Nb (100 nm)/Gd (3 nm)/V (70 nm)/Nb (15 nm)

Al_2O_3/Nb (100 nm)/Gd (6 nm)/V (70 nm)/Nb (15 nm)

Al_2O_3/Nb (100 nm)/Gd (12 nm)/V (70 nm)/Nb (15 nm)

Task 5

As to this task, reflectivity of neutron as well as X-Ray were simulated with variations of ferromagnetic layers. There are 5 ferromagnets assumed to exist in middle layers in each simulation (Gd, Fe, Co, Ni, Dy). It was assumed that there were no magnetizations and grazing angle was constant, 6 mrad. Because each element has differing neutron scattering length density, it was necessary to input neutron scattering length density for each element. Data for neutron scattering length density was obtained from Neutron Activation and Scattering Calculator (nist.gov) for this task, neutron scattering length density could be summarized as follow,

Elements	**Scattering Length Density (10^{-6}/Å^2)**
Gd	(obtained from lemur program) / 4.150
Fe	8.024
Co	2.265
Ni	9.408
Dy	5.356

The layers being used for this task were as follow,

Al_2O_3/Nb (100 nm)/Gd (3 nm)/V (70 nm)/Nb (15 nm)

Al_2O_3/Nb (100 nm)/Fe (3 nm)/V (70 nm)/Nb (15 nm)

Al_2O_3/Nb (100 nm)/Co (3 nm)/V (70 nm)/Nb (15 nm)

Al_2O_3/Nb (100 nm)/NI (3 nm)/V (70 nm)/Nb (15 nm)

Al_2O_3/Nb (100 nm)/Dy (3 nm)/V (70 nm)/Nb (15 nm)

Task 6

Task 6 concerned about comparing neutron and X-Ray reflectivity of superlattices (heterostructures with multiple repeating layers) with respect to the number of layers of the superlattices. It was assumed that there was no magnetization, and the grazing angle were constant 6 mrad. The superlattices variations were:

Al_2O_3/ [Nb(25nm) / Gd(3nm)] x10 / Nb(15nm)

Al_2O_3/ [Nb(25nm) / Gd(3nm)] x20 / Nb(15nm)

Al_2O_3/ [Nb(25nm) / Gd(3nm)] x30 / Nb(15nm)

Task 7

Task 7 compared roughness of heterostructures supercluster layers (20 layers) and how it would affect X-Ray reflectivity. The roughness was assumed for Gd layers with the value of 0, 1, 2, and 3 nm. For this task, it was assumed that grazing angles of X-Ray constant (6 mrad) and that there was no magnetization involved (zero field). For this task, it was assumed that the layers of the sample were,

Al_2O_3/ [Nb(25nm) / Gd(3nm)] x20 / Nb(15nm)

Task 8

In the last task, neutron reflectometry for helicoidal magnetization for heterostructures superclusters (20 layers) were being compared for several variations of magnetization value. It was assumed that in this task the grazing angle were constant for each simulation, 6 mrad. The variations were independently chosen by author to reflect the effect of helicoidal magnetization and reflectivity. The variables were,

Case	M_x (Oe)	M_y (Oe)	M_z (Oe)
1	1000	1000	1000
2	1000	1000	10000
3	100	100	1000
4	500	500	1000
5	10000	10000	1000

The reason why M_x and M_y has similar values were because in helicoidal structure, magnetization in each supercluster layer rotate for each layer and has same magnetization in x-y direction and constant "twist" in z-direction. In the following figure, it was simulated how the magnetization would look if it turned 360 degrees in 20 layers of heterostructures and how it would look if it turned 720 degrees in 100 layers of heterostructures

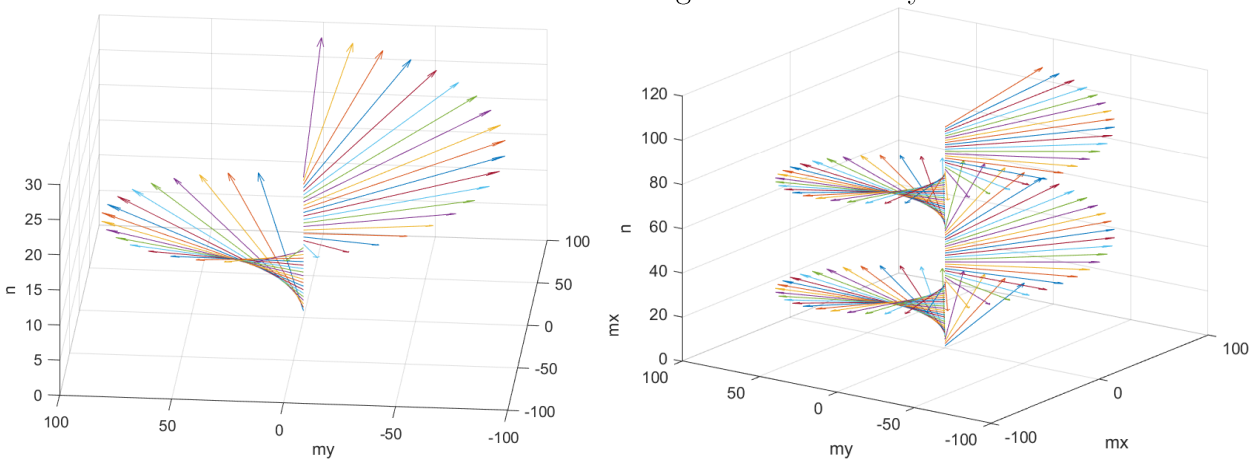

In this task, it was assumed that the layers (and Dy has 20 layers) were like,

Al2O3 / Nb(100nm) / Dy(3nm) / V(70nm) / Nb(15nm)

Results and Discussion

Task 1

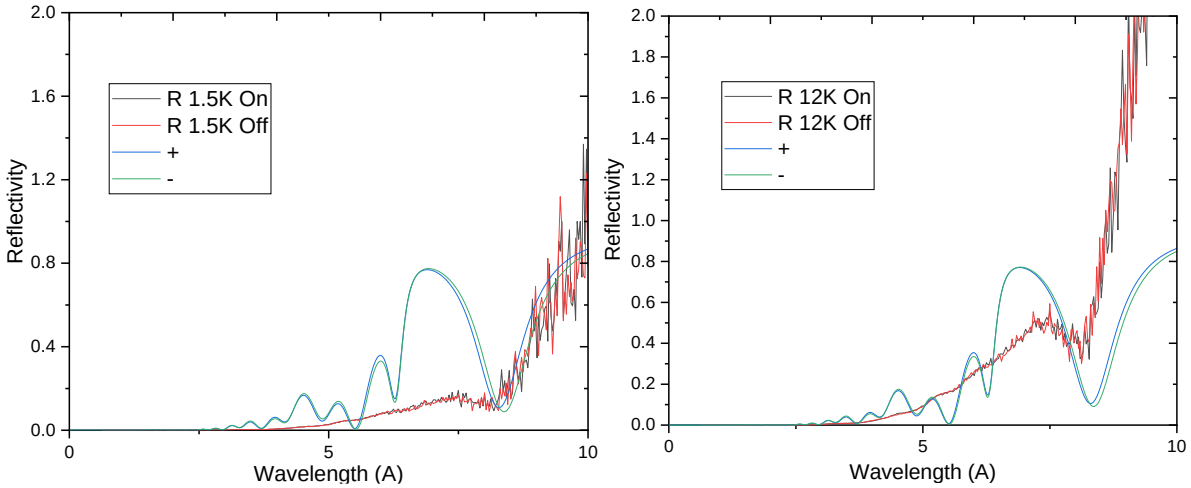

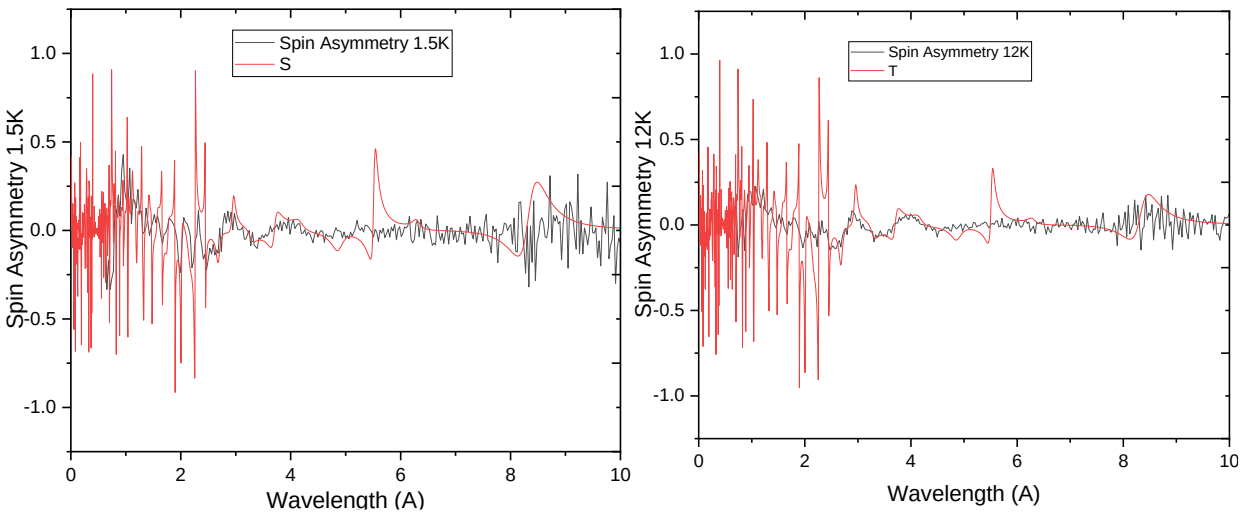

The above layers were simulated by assuming that in superconducting temperature, there is ferromagnetism in V and Nb layers with proximity layers with the width of 100 Angstrom, while in non-superconducting state, there was no additional layers of V and Nb and it was assumed hat magnetization of Gd at that temperature was around 3000 Oe. The difference between experimental data and simulation happened due to systematic error in simulation, hampered by insufficient information on the initial value of Nb and V thickness. Nonetheless, spin asymmetry of experimental result and simulation closely matched and due to differing asymmetry value in either case, it was assumed that spin asymmetry value arises in superconductivity layers due to ferromagnetic suppression of Gd layers.

Task 2

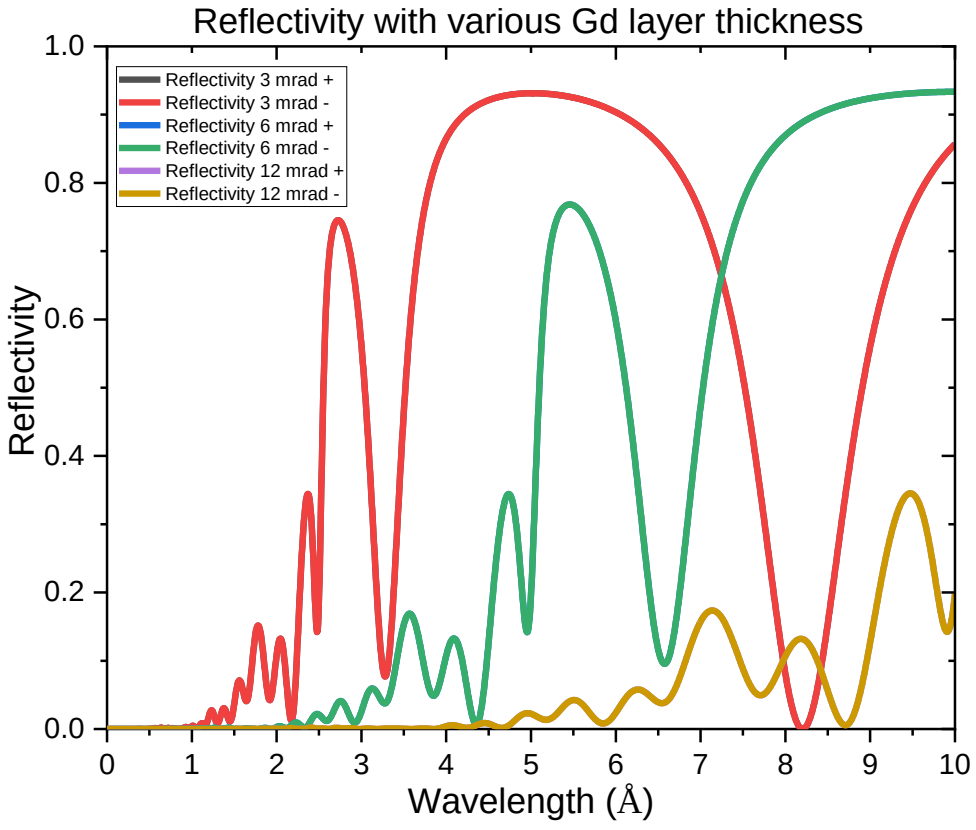

The figure for Task 7. Simulation results of reflectivity for various angles variations.

The result of the second task shows that for a wavelength from 1 to 10 Angstrom, there are variations of reflectivity of the samples when being varied with grazing angles. There were no differences in reflectivity of normal spin state (+) and spin flipped state (-) because varying the grazing angle did not changing the interaction between the beam or flipped beam and the sample. From the results above, we noticed that for a larger wavelength, we observed larger reflectivity which is consistent with small angle experiment where scattering intensity is exponentially inverse to $\mathbf{q}$ where $\mathbf{q}=\mathbf{2\pi/\lambda}$. However, upon closer look, we noticed that a smaller grazing angle results in a higher reflectivity. It could be easily described from Bragg's scattering equation where $2\,d\sin(\theta) = n\lambda$. If we noticed closely, for a smaller angle, then Bragg's equation can be satisfied for a rather larger d value. The heterostructures being simulated this time has a rather large size in nanometer-scale thus for this heterostructures, it was imperative to employ a smaller grazing angle to obtain higher value of reflectivity.

Task 3

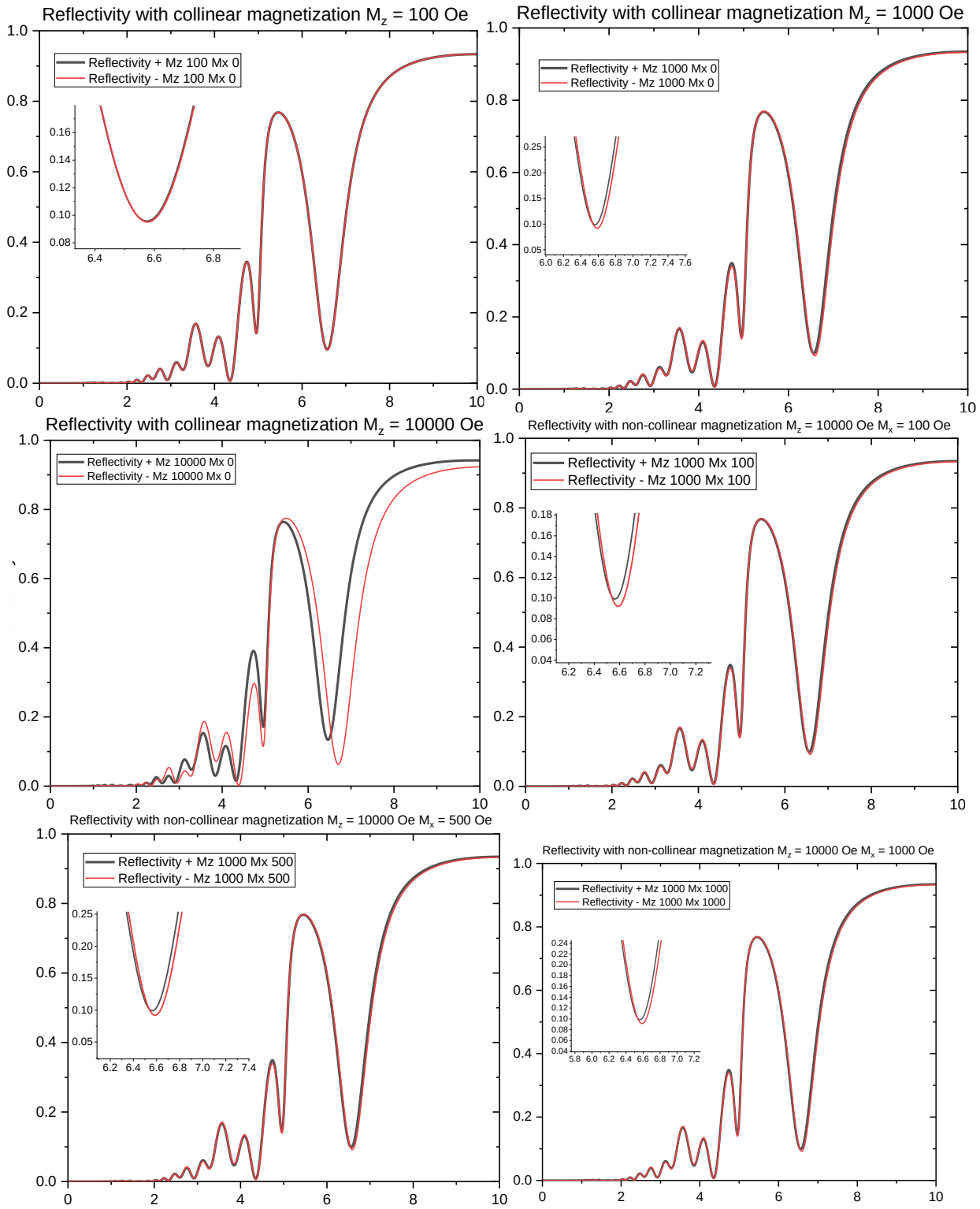

Figure Task 12. Simulation results for collinear and non-collinear cases.

The results above told us that for non-collinear cases, there is a small relative reflectivity shift of + state and – state for all variations. On the other hand, for collinear case there is no shift in reflectivity for small magnetic field. For large field, however, there is a shift between + states and – states because in large field, Zeeman splitting of spin states occurred and thus causing chiral spin states in the ferromagnet. For even larger field, larger shift was

observed. Magnetization of the sample is large enough to cause spin flip of scattered neutron beam.

Task 4

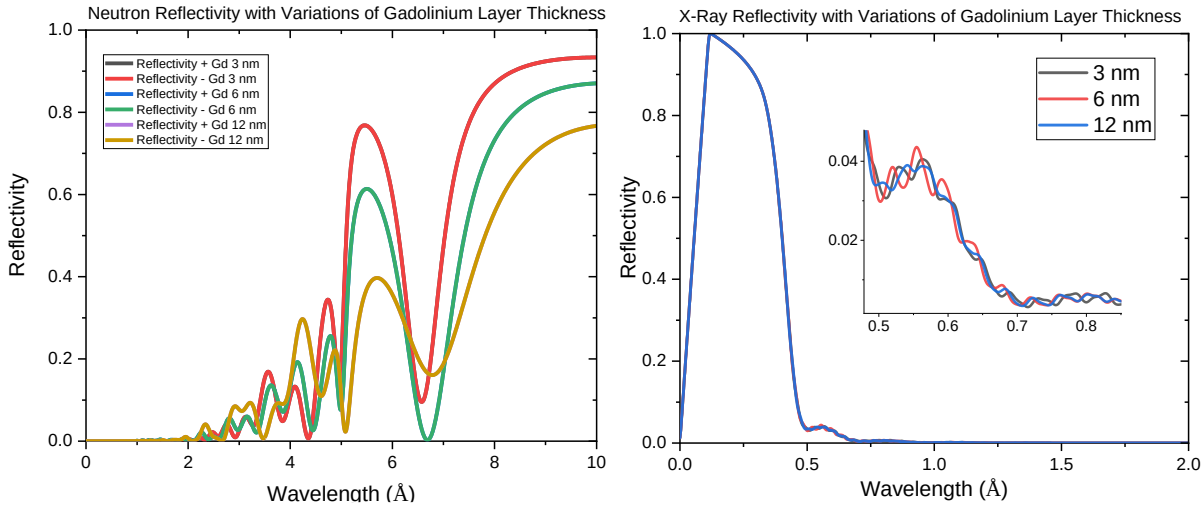

Figure Task 4. Simulation results of task 4 for both neutron and X-Ray beams.

Neutron reflectivity of Gd due to thickness variations showing a surprising result. The neutron reflectivity is suppressed for a larger value of thickness. This could be explained by knowing that for a larger value of thickness, superconducting order parameter inside Gd reached a deeper part of Gd and as such Cooper pair coherence caused more electron to be correlated to cooper pair in superconductors. As such, superconducting layer become thicker and as such it screens ferromagnetic response of Gd layer. On the other hand, X-Ray reflectivity does not change much if we added the thickness of Gd layer. This was explained by the fact that Gd layer in the middle of heterostructures does not contribute much to x-ray scattering, which mainly occurred at the surface. Since we know that X-Ray does not penetrate deeply inside metal then we could safely if addition of thickness of Gd layer does not contribute much to scattering. Another results that worth to mention was no + state and − variations observed in neutron beam simulation since we know that adding more thickness did not change beam interaction with the heterostructures.

Task 5

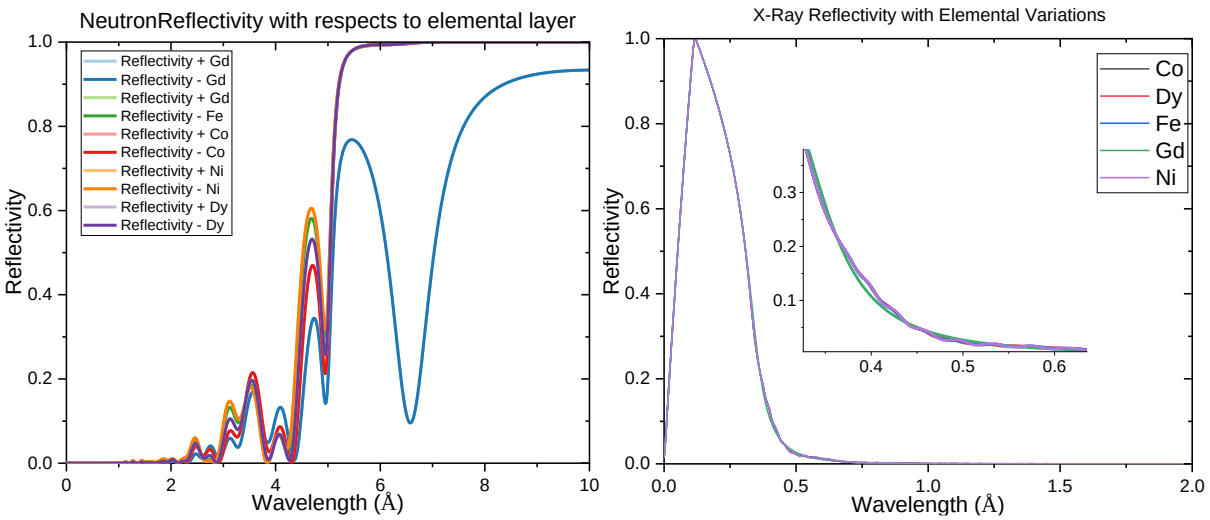

Figure Task 5. Simulation results of neutron and x-ray reflectivity.

The simulations shows that there is no noticeable x-ray reflectivity due to elemental variations. As explained previously, this can be attributed to location of the elements which was in the middle of heterostructures and because of that it did not contribute significantly to x-ray scattering. On the other hand, Neutron reflectivity has variational reflectivity in each peak of the upper left figure. Variational reflectivity below 5 Angstrom happened because ferromagnetism in the layer had various magnetic moment values. As such it has differing effect on proximity effect in the superconductivity. Gadolinium has a different neutron reflectivity value because in Gd/Nb layer, $E_F \sim E_S$ and as such allow rather a large proximity effect where Gadolinium has superconductivity inside it. As a result, it screened out incoming neutron and has lower reflectivity.

Task 6

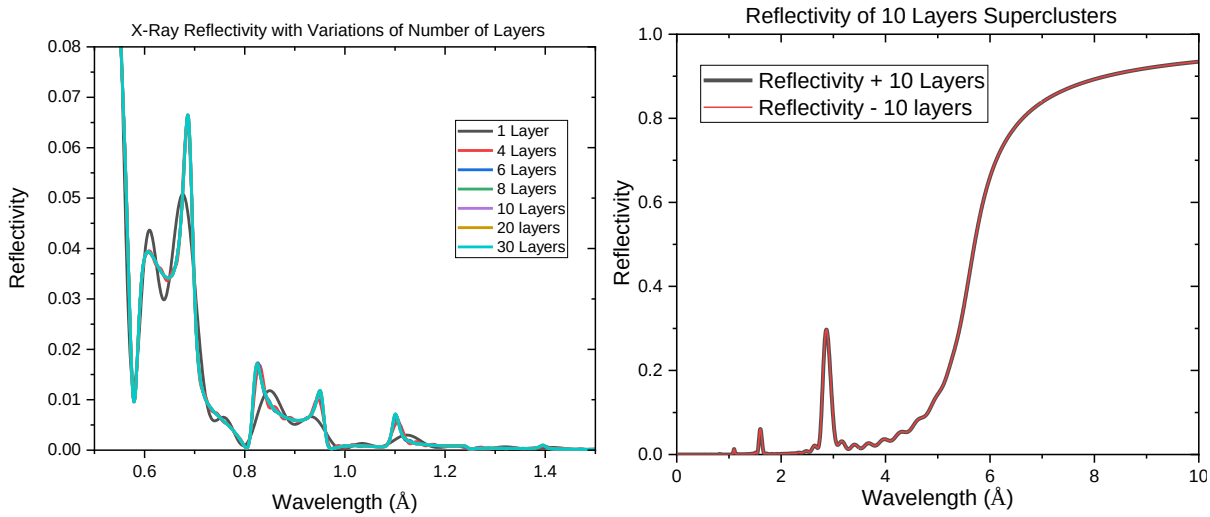

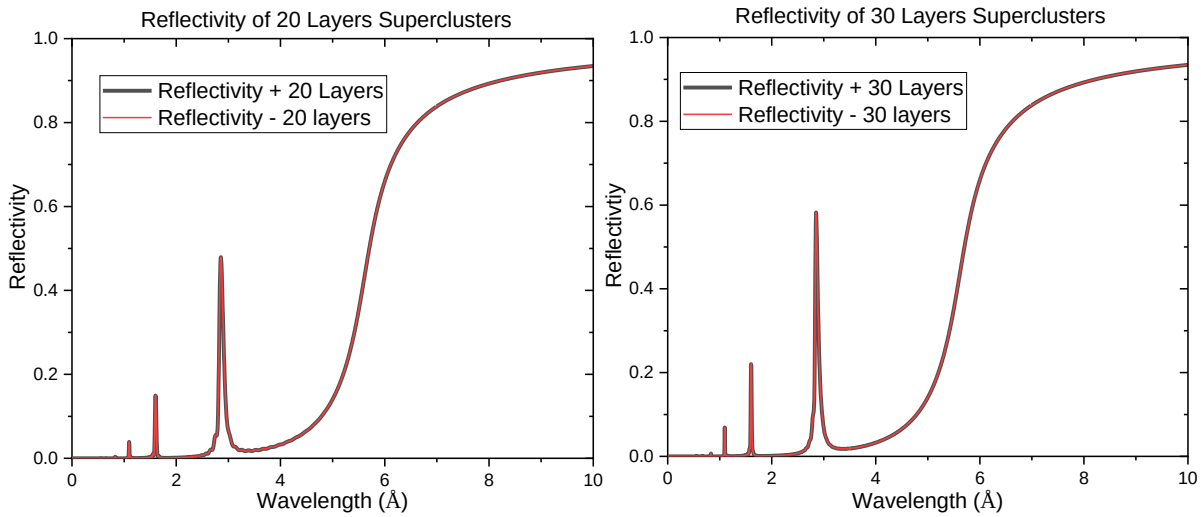

Figure for task 6. Simulated results of reflectivity for heterostructures superclusters. Upper left is for X-Ray beam and the rests are neutron beam.

X-Ray reflectivity showed an interesting result. A layer of heterostructures has different reflectivity than multiple layers (superclusters) of heterostructures. Upper figure showed that for multiple layers (4 and beyond), there are no significant changes in reflectivity intensity, but they had a larger reflectivity value compared to a layer of heterostructures. This happened because X-Ray scattering depended on electronic density on the surface of the sample. The larger the number of electrons, then we could expect that there should be a larger value scattered beam intensity. Furthermore, adding more layers to the samples means that there were more beams to reflect X-Ray, hence we found larger reflectivity value for multiple layers samples.

The reason why we didn't observe any variations of reflectivity with the addition of more layers had to do with X-Ray penetration depth which was quite low for a sample that has large surface electronic density of states such as transition metal. In contrast with X-Ray, the addition of more heterostructures layers gave rise to a larger value of reflectivity because neutron has a larger penetration depth than X-Ray (it does not interact with electron cloud around nucleus), as such when we add more layers to the samples, then we would expect to have more nuclear magnetic moment which could scatter neutron. The result is consistent with what we already know so far about neutron and its behaviors.

Task 7

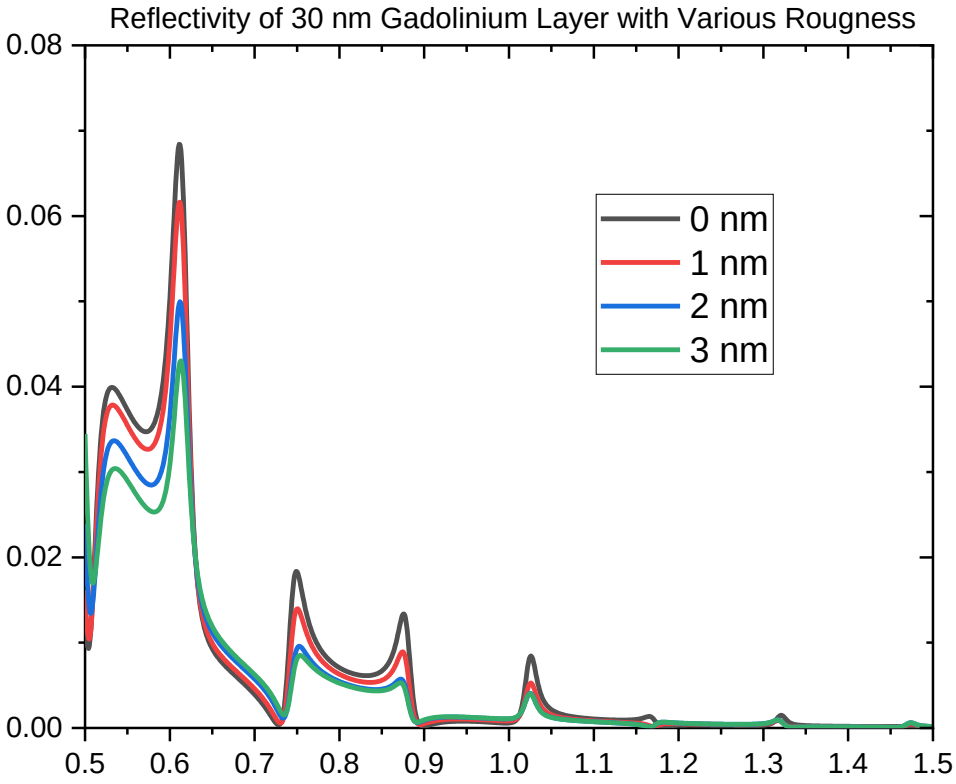

Figure Task 7. Simulation results of task 7.

The simulation of x-ray reflectivity of gadolinium layer with various roughness is closely matched theoretical prediction of X-Ray reflectivity. From the figure, we could observe that from 0.5 to 1.5 Angstrom, reflectivity of each sample varied with several noticeable peaks at 0.55, 0.66, 0.75. 0.9, and 1.025 Angstrom. For a small angle scattering, intensity of scattered beam decreased exponentially for a larger beam wavelength. This happened because from Bragg's equation of scattering, a coherent scattering only occurs if and only if beam wavelength has some correspondence with object being observed, so for a larger wavelength, scattered beam would have a lowered intensity.

X-Ray scattering experiment often relied from the fact that detectors could only detect scattered beam that arrived at it, including superposition of beam due to lattice scattering of multilayers samples. If samples have some defects or inhomogeneity, then scattered beam would display reduced intensity because destructive interference of reflected beam. This explains why in the results above, for a larger value of roughness, reflectivity became smaller. The reason is because for a larger value of roughness more beam were getting destructive interference and at the same time scattered specularly to more direction, thus reducing intensity of beams that arrived at the sample.

Task 8

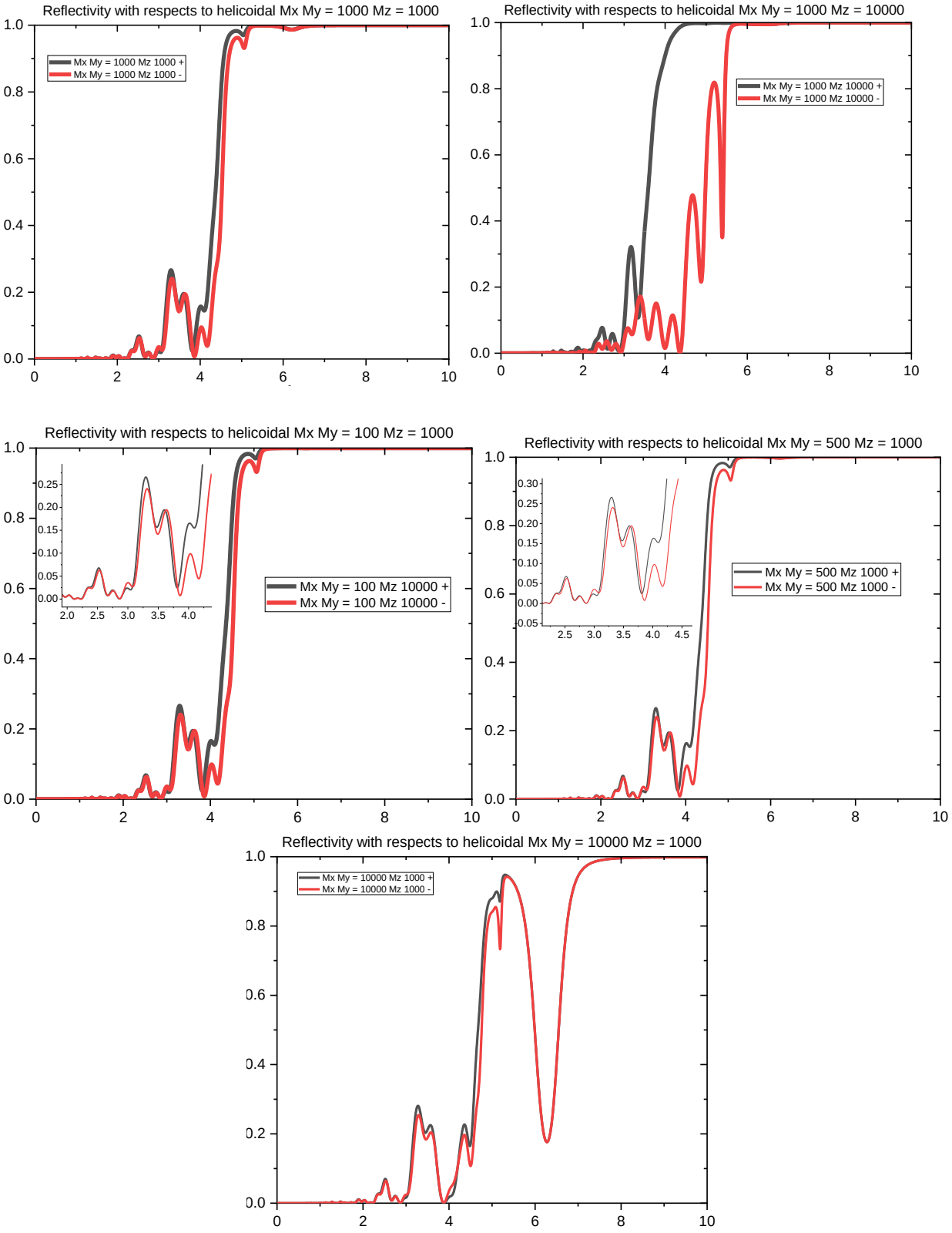

Figure Task 8. Simulation results for helicoidal magnetizations variations.

As could be seen above, Dysprosium layer which is not ferromagnetic but *helimagnetic* showed an interesting result. Variations of small moment in x and y direction did not affect reflectivity but the addition of more magnetization both in z direction and xy-direction significantly changed reflectivity. Because Dysprosium is a helimagnet, then its

spin was revolved around in xy and has constant moment in z direction, forming helical magnetization. Since spin revolution in Dy is a chiral quantity, then when it received neutron beam, the reflected beam intensity would also depend on the state of the beam's spin. As a result, it showed prominent different reflectivity value between + state and – state.

References

[1] Mildred Dresselhaus (1999), Lecture notes on superconductivity and solid-state physics

[2] R. Kleiner and W. Buckel, (n.d.).

[3] M. Tinkham, **1**, 102 (2004).

[4] P. W. Anderson and H. Suhl, Physical Review **116**, 898 (1959).

[5] A. I. Buzdin, Reviews of Modern Physics **77**, 935 (2005).

[6] V. Yagovtsev, N. Pugach, and M. Eschrig, Superconductor Science and Technology **34**, (2020).

[7] V. D. Zhaketov *et al.*, (2021).

[8] J. Stahn *et al.*, Physical Review B - Condensed Matter and Materials Physics **71**, 140509 (2005).

[9] Y. N. Khaydukov *et al.*, Physical Review B **99**, 140503 (2019).

[10] D. I. Devyaterikov *et al.*, Physics of Metals and Metallography **122**, 465 (2021).

[11] V. D. Zhaketov *et al.*, Journal of Experimental and Theoretical Physics **129**, 258 (2019).

[12] Y. N. Khaydukov *et al.*, JETP Letters 2013 98:2 **98**, 107 (2013).